Electronic Supplementary Material (ESI) for Nanoscale.

`

†Electronic Supplementary Information

High-Resolution, Electrohydrodynamic Inkjet Printing of Stretchable, Metal Oxide Semiconductor Transistors with High Performances

S.-Y. Kim,[a] K. Kim,[a] Y.H. Hwang,[b] J. Park,[a] J. Jang,[a] Y. Nam,[c] Y. Kang,[d] M. Kim,[a] H. J. Park,[a] Z. Lee,[a] J. Choi,[d] Y. Kim,[e] S. Jeong,[f] B.-S. Bae[*c] and J.-U. Park[*a]

[a.] School of Materials Science and Engineering, Ulsan National Institute of Science and Technology (UNIST), Ulsan Metropolitan City, 44919, Republic of Korea.
Email: jangung@unist.ac.kr

[b.] Radiation and Environmental Lab., Central Research Institute, Korea Hydro and Nuclear Power, Daejeon Metropolitan City, 34114, Republic of Korea

[c.] Department of Materials Science and Engineering, Korea Advanced Institute of Science and Technology (KAIST), Daejeon Metropolitan City, 34141, Republic of Korea.
Email: bsbae@kaist.ac.kr

[d.] School of Electrical and Computer Engineering, Ulsan National Institute of Science and Technology (UNIST), Ulsan Metropolitan City, 44919, Republic of Korea.

[e.] Department of Computer Engineering, Kwangwoon University, Seoul Metropolitan City, 01897, Republic of Korea.

[f.] Division of Advanced Materials, Korea Research Institute of Chemical Technology (KRICT), Daejeon Metropolitan City, 34114, Republic of Korea.

`

Experimental Section

Indium oxide (In_2O_3) precursor solution synthesis

An aqueous indium oxide (In_2O_3) precursor solution was synthesized by dissolving indium nitrate hydrate ($In(NO_3)_3$-xH_2O, 99.999% Sigma-Aldrich) in deionized water. The total molar concentration of the In_2O_3 solutions was 0.2M. The solution was stirred at the ambient atmosphere for 6 hrs.

Zr-doped AlOx (ZAO) synthesis and fabrication of ZAO dielectric layers

For the Zr-doped aluminum oxide film (ZAO), aluminum chloride ($AlCl_3$, 99.999%, Sigma-Aldrich) and zirconium chloride ($ZrCl_4$, 99.99%, Sigma-Aldrich) were dissolved in a mixture of acetonitrile (CH_3CN, 99.8%, Sigma-Aldrich) and ethylene glycol ($HOCH_2CH_2OH$, 99.8%, Sigma-Aldrich) with a 35/65 volume ratio. The molar concentration of the solutions was 0.4 M. The solution preparation processes were conducted in N_2 condition. As a substrate, a heavily boron-doped silicon wafer (p^+-type Si) was used after cleaning in an ultrasonic bath. The ZAO precursor solution were spun at 3000 rpm for 25 s and directly annealed at 250 ºC in hot plate for 120 min. The spin coating and annealing steps were repeated 4 times to achieve the desired thickness of 155nm. According to our previous reports on *C-f* measurement of the solution-processed high-*k* dielectrics at low-frequency region[49], the dielectric constant of the ZAO layer is measured 21.7 at 100 Hz.

Preparation of the 1.8 µm-thick PI substrate

After poly(methyl methacrylate) (PMMA) which act as a sacrificial layer was spun at 1000 rpm for 30 s on a Si wafer, the PI solution was spun at 3000 rpm for 30 s. Thermal curing process for PI solution was conducted at 250 ºC for 4 hrs. After the polyimidization of the PI susbstrate, the PMMA layer was dissolved by soaking in acetone for 15 min and the remaining PI film was peeled off from the Si wafer.

Characterization of the e-jet printed In_2O_3 film and TFTs

To analyze surface morphology and thickness profile of the e-jet printed layer, atomic force microscopy (AFM, DI-3100) was performed with a non-contact mode. The chemical composition of the printed layer (at PPM and NPM) and spun layer was examined by X-ray photoelectron spectroscopy (XPS, K-Alpha). Cross-sectional image and diffraction pattern of the In_2O_3/ZAO interface was analyzed by transmission elelectron microscopy (TEM, JEOL-2100F). Transfer and output characteristics and stability of TFTs and electrical properties of the amplifier were measured by a Keithley 4200-SCS semiconductor parametric analyzer.

Fabrication of common-source amplifier

For the fabrication of the common-source amplifier, Cr 3nm/Au 80nm was deposited on SiO_2 300 nm wafer and photo-lithographically patterned to form a gate electrode. The preparation of a 155nm thick layer of ZAO dielectrics is described in the ESI Experimental Section. To get access to the gate contact pads, vias were formed by etching solution of H_3PO_4 (55-56%), Sodium m-nitrobenzene sulfonate (5-10%) and $C_2H_4O_2$ (1-5%). After e-jet print In_2O_3 (width: 100 μm, length: 50 μm) and subsequent annealing process, Au electrode (thickness: 100 nm drain) was photolithographically patterned as source/drain electrode. The fabrication was finished by the photolithographical patterning of the 15 nm-thick ITO as resistive load.

`

Supplementary Table

Ref.	Method	material	μ ($cm^2 V^{-1} s^{1}$)	Temp. (℃)	Advanced researches
37	E-jet	IZO	3.7	500	Transparent TFTs on glass
38	E-jet	ZTO	9.8	500	-
25	E-jet	IGZO	1.3	400	-
15	Ink-jet	IGZO	0.03	450	-
5	Ink-jet	In_2O_3	6	200	-
27	Ik-jet	In_2O_3	3.98	200	-
31	Ink-jet	ZnO	1.61	250	1) Inverter 2) Flexible TFTs
33	Flexography	In_2O_3	8	300	-
40	Spray pyrolysis	Li-doped ZnO	85	400	
Our results	E-jet	In_2O_3	222	250	1) Printed In_2O_3 TFTs with e-jet printing-assisted high-resolution S/D electrodes 2) Logic circuits 3) E-jet printing of encapsulation layer 4) Flexible/stretchable TFT

Table S1 Comparison our results with previous reports

`

Ref.	Material	Novelty	Disadvantages
37	IZO	1) Use of e-jet printing for the fabrication of metal oxide TFTs 2) High resolution e-jet printing (line width: 1.5 μm)	1) Low mobility (3.7 $cm^2 V^{-1} s^1$) 2) High-temperature process (500°C) which limits the use of plastic substrates
38	ZTO	1) Use of e-jet printing for the fabrication of metal oxide TFTs	1) Low mobility (9.8 $cm^2 V^{-1} s^1$) 2) Low resolution inkjet printing (line width: 60 μm) 3) High-temperature process (500°C) which limits the use of plastic substrates
25	IGZO	1) IGZO ink incorporating formamide to enhance the mobility 2) Use of e-jet printing for the fabrication of metal oxide TFTs	1) Low mobility (1.3 $cm^2 V^{-1} s^1$) of the e-jet printed TFTs 2) High-temperature process (400°C) which limits the use of plastic substrates
15	IGZO	1) Use of inkjet printing for the fabrication of metal oxide TFTs	1) Low mobility (0.03 $cm^2 V^{-1} s^1$) 2) Low resolution inkjet printing (droplet diameter: 40 μm) 3) high-temperature process (450°C) which limits the use of plastic substrates
35	In_2O_3	1) Use of inkjet printing for the fabrication of metal oxide TFTs 2) Low annealing temperature (< 200°C)	1) Low mobility (3.98 $cm^2 V^{-1} s^1$) 2) Low resolution inkjet printing (droplet diameter: 300 μm) 3) Post annealing process to develop the bias stability
27	In_2O_3	1) Low temperature process (< 200°C) 2) Use of inkjet printing for the fabrication of metal oxide TFTs	1) Low resolution inkjet printing (line width: 500 μm)
31	ZnO	1) Use of inkjet printing for the fabrication of metal oxide TFTs 2) Low voltage operation (< 2 V) by using printed ion-gel electrolyte as gate dielectrics 3) Fabrication of the inverter 4) Fabrication of the flexible metal oxide TFTs	1) Low mobility (1.61 $cm^2 V^{-1} s^1$) 2) Low resolution inkjet printing (line width: 50 μm) 3) Use of the PEDOT:PSS as gate electrode which is not suitable for practical usage due to the poor long-term reliability
Our results	In_2O_3	1) Use of e-jet printing for the fabrication of metal oxide TFTs 2) High resolution e-jet printing (line width: 2 μm) 3) Transistors with a high mobility of 222 $cm^2 V^{-1} s^1$ by e-jet printing process 4) Enhancement of the bias stability by e-jet printing of encapsulation layer 5) Fabrication of the logic circuits 6) E-jet printed metal oxide TFTs with e-jet assisted high-resolution electrode 7) Fabrication of flexible/stretchable metal oxide TFTs by using e-jet printing	

Table S2 Comparison our novelty with previous reports

`

Ref.	Methods	Mobility [$cm^2 V^{-1} s^{-1}$]	Temp. [°C]	application
32	Inkjet printing of IZO on high-k dielectrics (Zr doped AlO_x)	54.2	350	-
40	Spray pyrolysised TFTs based on Li-doped ZnO semiconductor and ZrO_2 dielectrics	85	400	-
49	Use of a-IGZO incorporating AgNWs as active channel layer	174	400	-
50	Use of Ca/Al-capped a-IGZO as channel layer	160	400	-
Our results	E-jet printing In_2O_3 on high-k dielectrics (Zr doped AlO_x)	222	250	Logic circuits

Table S3 Comparison our results with previous reports which have focused on dramatic enhancement of the mobility value

`

Supplementary Figures

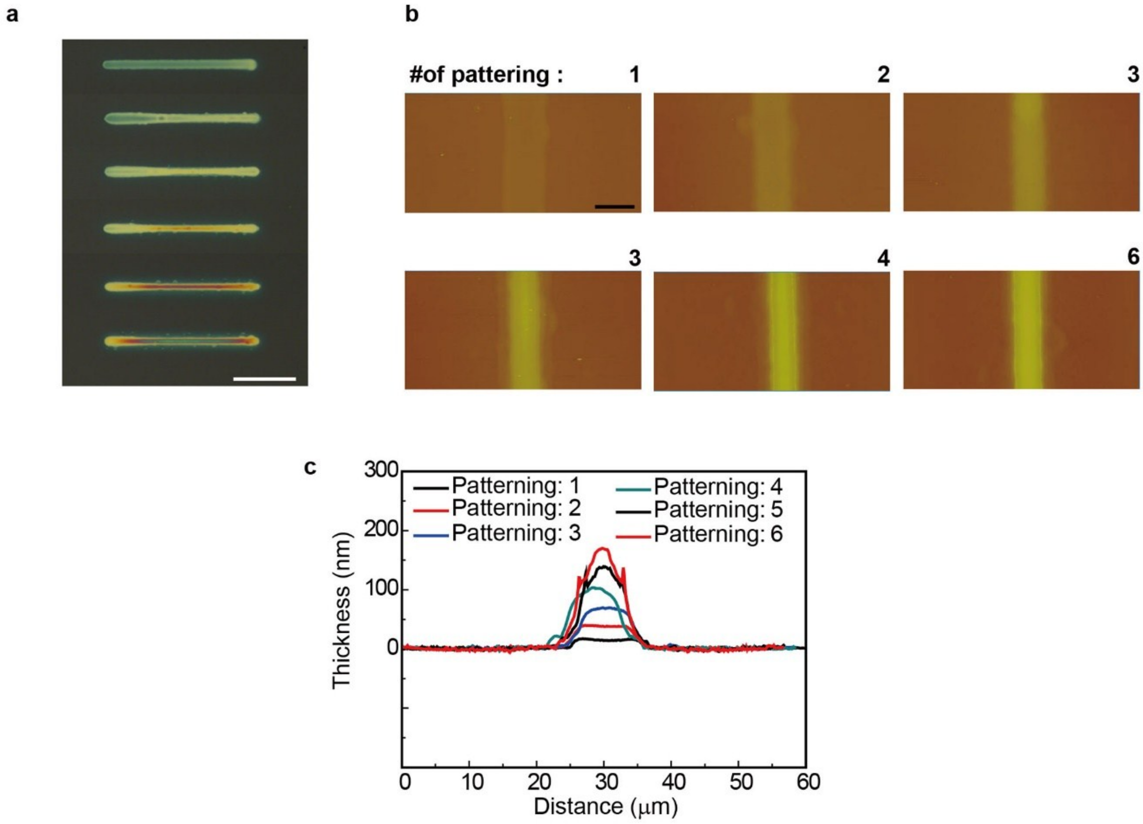

Fig. S1 Controllable thickness of MOS layers by e-jet printing. (a) Optical micrograph, (b) AFM images and (c) two-dimensional profiles of various thickness of printed layers. White scale bar, 100 μm. Black scale bar, 10 μm.

`

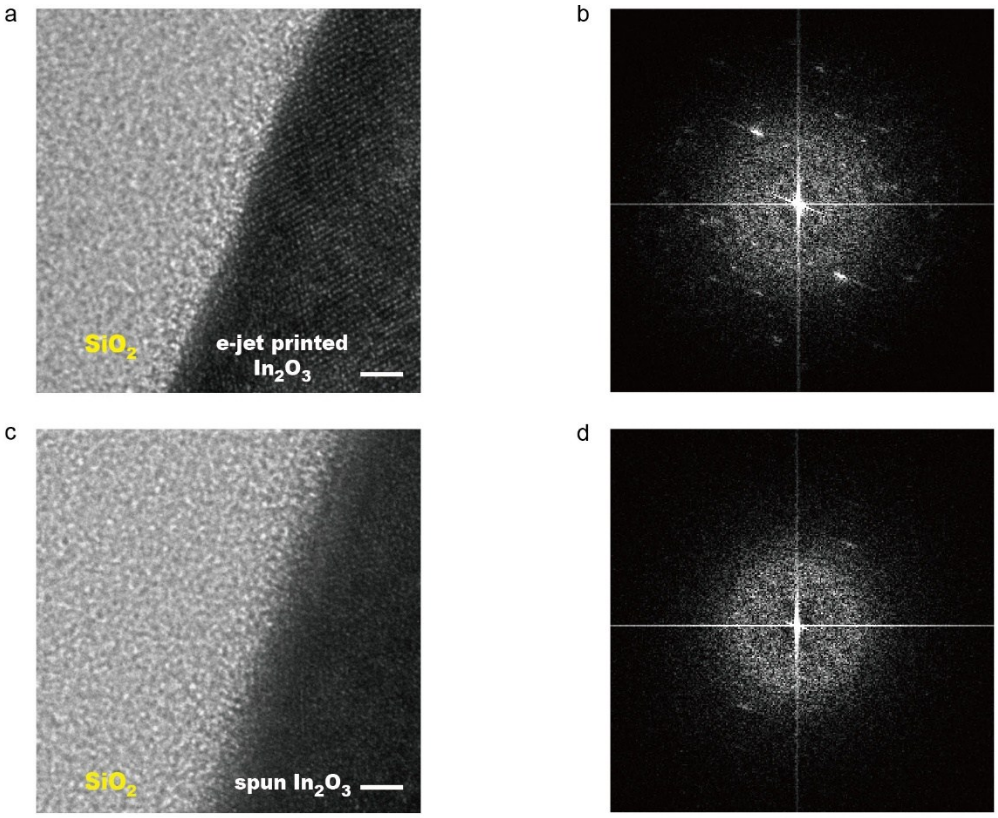

Fig. S2 Film properties of e-jet printed and spun In_2O_3 layer on SiO_2 dielectrics. High-resolution transmission electron microscope (TEM) image (a) and diffraction pattern (b) of selective area in e-jet printed layer, showing nano-crystalline phase in the overall film. TEM image (c) and diffraction pattern (d) of selective area in spun layer, showing amorphous phase and clusters in the film. White

`

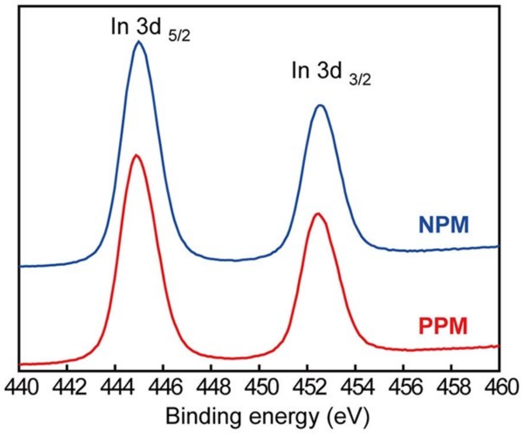

Fig. S3 XPS analysis of In3d peak in the In_2O_3 followed by e-jet printing with NPM and PPM. In3$d_{5/2}$ XPS spectra of In2O3 films printed by both PPM and NPM indicates the indium species in printed layer are in oxidation states with In-O bonds.

`

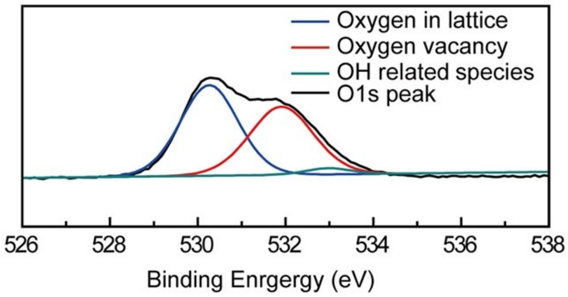

Fig. S4 XPS analysis of O1s peak in the In_2O_3 followed by spin coating. O1s XPS spectra of the In_2O_3 films formed by spincoating, which are deconvoluted by O_{OX}, O_V, and O_{OH} sub-curves, exhibiting peaks at 530, 532 and 534 eV, respectively.

`

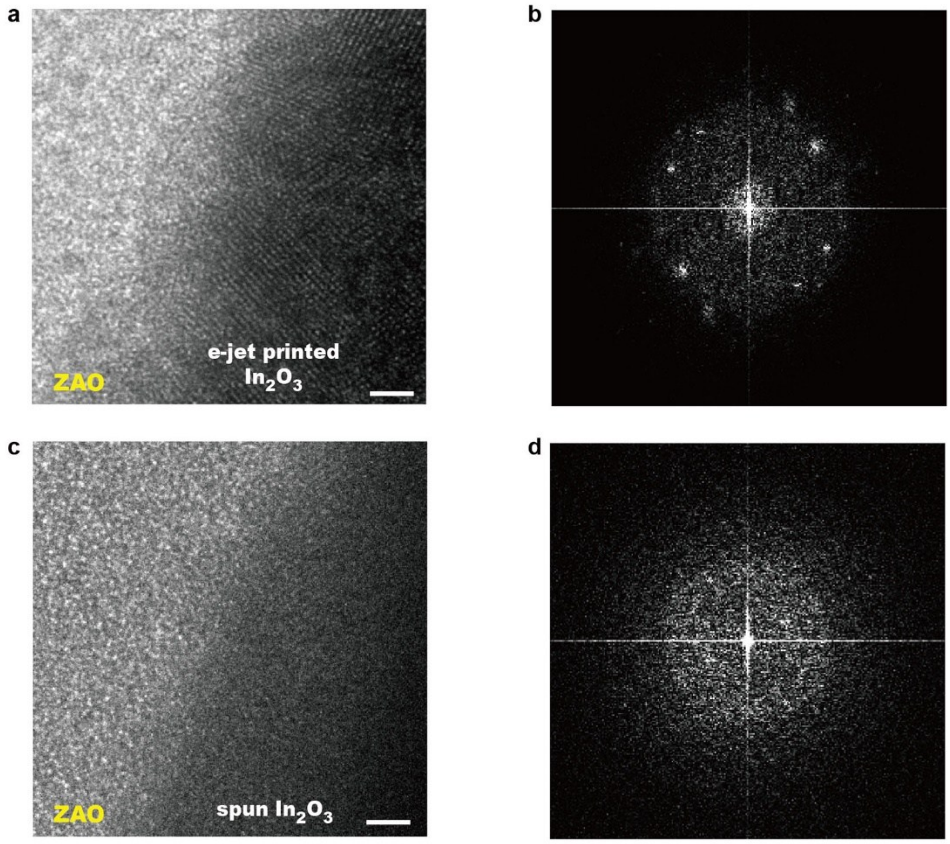

Fig. S5 Film properties of e-jet printed and spun In_2O_3 layer on ZAO dielectrics. High-resolution TEM image (a) and diffraction pattern (b) of selective area in e-jet printed layer. The TEM image exhibits nano-crystalline phase in the overall film and gradual transition from ZAO dielectrics to printed In_2O_3 layer. High-resolution TEM image (c) and diffraction pattern (d) of selective area in spun layer. The TEM image shows amorphous phase and clusters in the film. White scale bar, 2 nm.

`

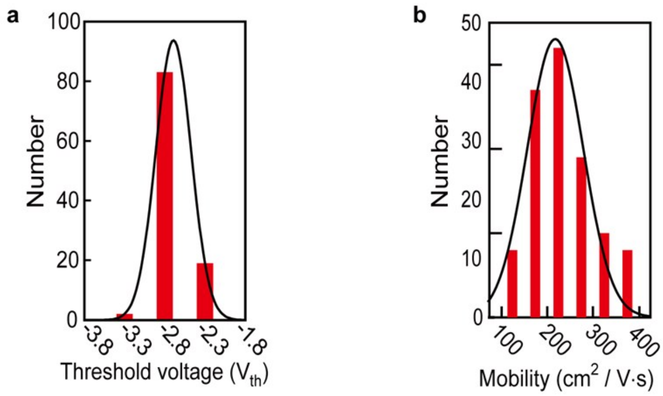

Fig. S6 Statistical distribution of e-jet printed TFTs employing ZAO dielectrics in linear regime (V_d = 1 V). (a) Mobility and (b) Threshold voltage of the 100 devices.

`

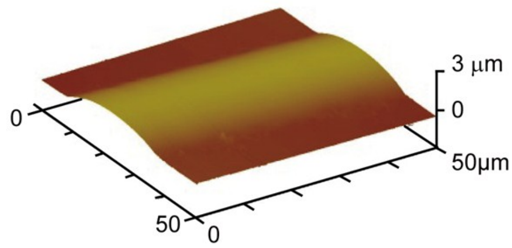

Fig. S7 AFM image of printed passivation layer. This AFM image shows that the entire printed channel region is encapsulated by e-jet printing of inorganic-organic hybrid precursor based passivation layer.

`

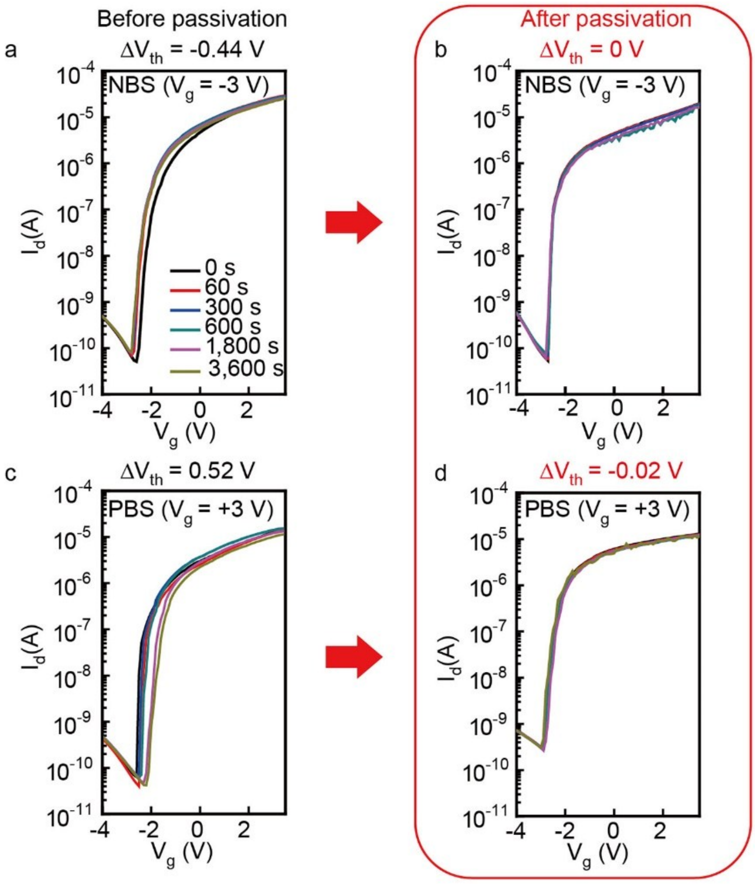

Fig. S8 Transfer characteristics of TFTs stressed for 3600 s under negative gate bias (NBS) and positive gate bias (PBS) with/without passivation layer (V_g = ± 3 V and V_d = 1 V). TFT characteristics under NBS (a) without passivation layer and (b) with passivation layer, showing improved bias stability from ΔV_{th} = -0.44 V to ΔV_{th} = 0V. TFT characteristics under PBS (c) without passivation layer and (d) with passivation layer, showing improved bias stability from ΔV_{th} = 0.52 V to ΔV_{th} = -0.02 V.

`

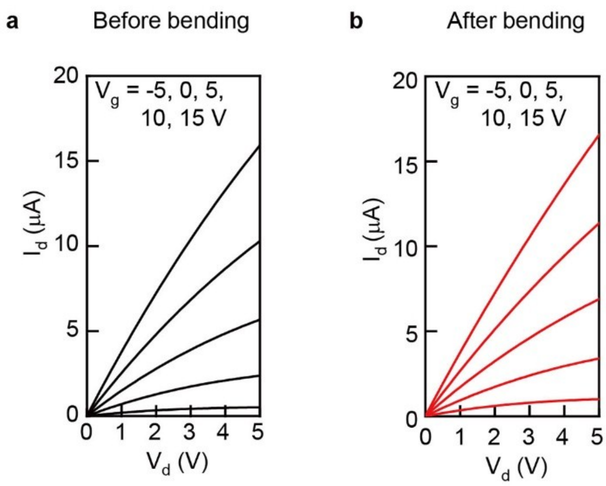

Fig. S9 Output characteristics of the flexible TFTs before and after transferring to the cylindrical curvature with radius of 3.5 mm. Output characteristics for V_g ranging from -5 V to 15 V in 5 V steps (a) before and (b) after bending to cylindrical support.

`

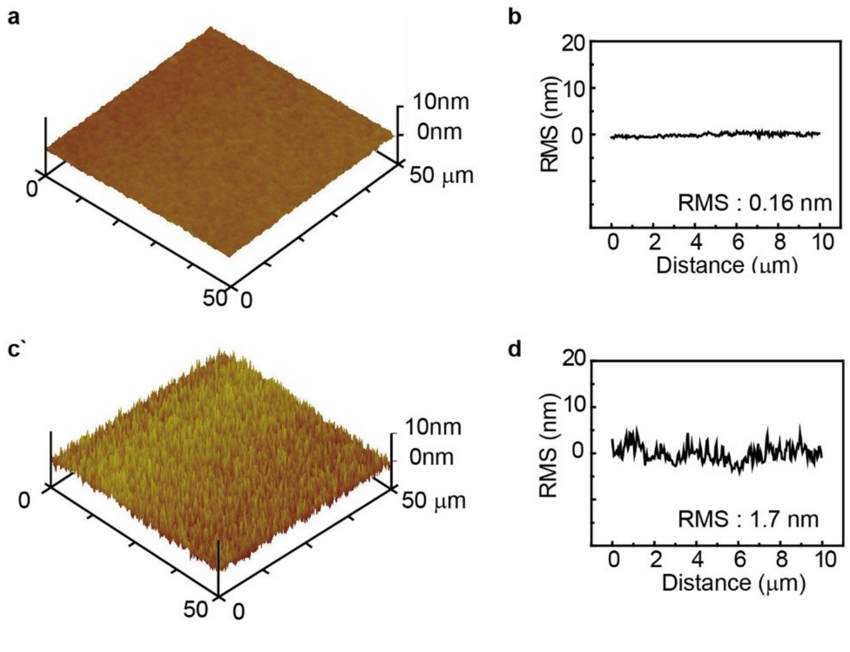

Fig. S10 Roughness of SiO_2 substrate and polyimide substrate. (a) AFM image and (b) RMS roughness of the surface of the SiO_2 substrate. (c) AFM image and (d) RMS roughness of the surface of the polyimide substrate.

`

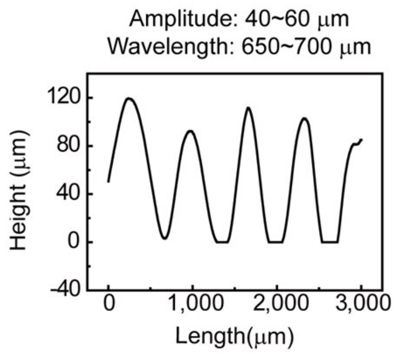

Fig. S11 The wave topology of stretchable, ultra-thin substrate characterized by α-step. After releasing of the ultra-thin PI substrate from pre-strain PDMS, stretchable PI substrate exhibit the wavelength and amplitude of wave of ~700 μm and ~50 μm, respectively.

`

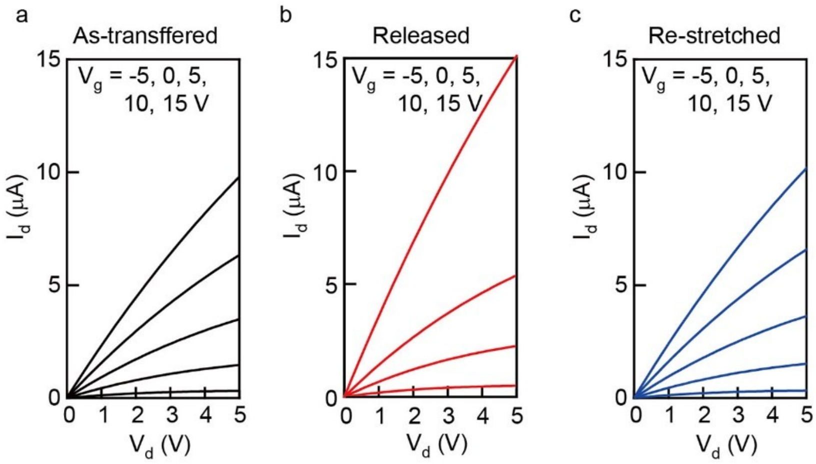

Fig. S12 Output characteristics of the stretchable TFTs corresponding to the states of the stretchable TFTs (V_g ranging from -5 V to 15 V in 5 V steps). Output characteristics (a) after TFT arrays sheet is as-transferred to the 10% pre-stretched PDMS, (b) after pre-stretched PDMS is relaxed, and (c) after relaxed PDMS is10% re-stretched.

`

Calculation of density of interface defect (D_{it})

The interface trap density (D_{it}) is one of the main dominants for transistor performance, which results in the large carrier scattering and trapping in the channel layer. According to the conventional metal oxide semiconductor field effect transistor, interface trap density can be calculated from the sub-threshold swing. We summarized the results of calculated density of the interface defect as follows:

Samples	Annealing Temp. (°C)	Capacitance (F cm^{-2})	μ (cm^2 V^{-1} s^{-1})	S (V per decade)	D_{it} (cm^{-2} eV^{-1})
E-jet printed In_2O_3 on ZAO	250	7.5X10^{-8}	222	0.2	**9.0X10^{11}**
E-jet printed In_2O_3 on SiO_2	250	3.7 X10^{-8}	7.7	1.2	**5.0X10^{12}**

$S = (\frac{d(log_{10}I_d)}{dV_g})^{-1} \approx ln10\frac{kT}{q}\left[1 + \frac{qD_{it}}{C_i}\right]$, where k: Boltzmann's constant, q: electronic charge, Ci:

Component materials and device performance parameters of metal oxide TFTs